Journal of Cancer Research and Clinical Oncology (2020) 146:1545–1558
https://doi.org/10.1007/s00432-020-03205-x

REVIEW – CLINICAL ONCOLOGY

Diagnostic approach in hepatic lymphoma: radiological imaging findings and literature review

Davide Ippolito[1,3] · Marco Porta[1,3] · Cesare Maino[1,3] · Anna Pecorelli[1,3] · Maria Ragusi[1,3] · Teresa Giandola[1,3] · Giulia Querques[1,3] · Cammillo Talei Franzesi[1,3] · Sandro Sironi[2,3]

Received: 12 February 2020 / Accepted: 30 March 2020 / Published online: 15 April 2020

Abstract

Purpose Imaging manifestations of hepatic lymphoma, both primary (PHL) and secondary (SHL), are extremely variable and non-specific, but some features are useful diagnostic clues in an appropriate clinical setting. Through a PubMed search, we found several published reviews focused on PHL and SHL diagnosis. However, to the best of our knowledge, few of them encompass a comprehensive analysis of all the diagnostic tools and relative radiological findings. The aim of this review is to provide a description of the radiological features of both PHL and SHL, by critically analyzing the available literature.

Materials and methods An extensive review of published literature along with a description of personal case series of both PHL and SHL has been conducted.

Results SHL can be easily diagnosed with imaging techniques, as it is usually associated with node disease. On the contrary the diagnosis can be a challenge in PHL, often mimicking HCC or liver metastasis of adenocarcinoma. In this context, multiparametric MRI plays a fundamental role in the differential diagnosis. Both for PHL and SHL, liver involvement presents as solitary or multiple lesions or as diffuse infiltrative disease.

Conclusion PHL and SHL may be correctly characterized using different radiological techniques. Both CT and MRI have showed a good correlation with histology, as they permit to distinguish between lymphomatous tissue, and necrotic and fibrotic areas.

Keywords Primary hepatic lymphoma · Secondary hepatic lymphoma · Computed tomography · Magnetic resonance imaging · Ultrasound

Abbreviations

ADC	Apparent diffusion coefficient
CEA	Carcinoembryonic antigen
CT	Computed tomography
DWI	Diffusion-weighted imaging
FDG	Fluoro deoxy glucose
Gd-BOPTA	Gadobenate dimeglumine (Multihance®)
Gd-EOB-DTPA	Gadolinium ethoxybenzyl diethylenetriamine pentacetic acid (Primovist®)
HCV	Hepatitis C virus
HCC	Hepatocellular carcinoma
HL	Hodgkin lymphoma
MRI	Magnetic resonance imaging
NHL	Non-Hodgkin lymphoma
PET	Positron emission tomography
PHL	Primary hepatic lymphoma
PTLD	Post-transplant lymphoproliferative disease
SHL	Secondary hepatic lymphoma
US	Ultra-sonography
αFP	αFeto-protein

Electronic supplementary material The online version of this article (https://doi.org/10.1007/s00432-020-03205-x) contains supplementary material, which is available to authorized users.

✉ Anna Pecorelli
pecorelli.anna@gmail.com

[1] Department of Diagnostic Radiology, H. S. Gerardo Monza, Via Pergolesi 33, 20900 Monza, MB, Italy

[2] Department of Diagnostic Radiology, ASST Papa Giovanni XXIII, Bergamo, Italy

[3] School of Medicine, University of Milano-Bicocca, Milan, Italy

Introduction

Lymphomas are the fifth most common cancers and the fifth leading causes of cancer mortality in the Western World, accounting for 4% of malignancies in adults and 21% in adolescents (Shanbhag and Ambinder 2018). Their pathogenesis relies on clonal neoplasms proliferation arising from B cell, T cell, and natural killer cell subsets at various stages of maturation (Elenitoba-Johnson and Lim 2018), and they are traditionally divided into Hodgkin lymphoma (HL) and Non-Hodgkin Lymphoma (NHL). Both HL and NHL can locate in sites other than the lymphatic system (nodes, spleen, thymus, tonsils, and pharyngeal lymphatic ring) and this condition is known as extranodal lymphoma. In general, extranodal involvement is more common in NHL than HL (20–40% vs 5%), with secondary forms being more prevalent (Leite et al. 2007). In NHL, which spreads via hematic supply to non-contiguous sites, the extranodal disease is often present at the time of diagnosis, appearing as a bulky retroperitoneal or mesenteric lymphadenopathy, potentially involving any organ including liver, bowel, pancreas, kidney, bone marrow, pelvic structures, and skin (Dalrymple et al. 2010). Therefore, since any abdomino-pelvic tissue may virtually be affected, the disease may present with a variety of symptoms that correspond to different imaging manifestations (Armitage et al. 2017). HL spreads through the lymphatics from one nodal group to contiguous ones, typically presenting as a supra-diaphragmatic disease. The more common sites of abdominal localization are paraaortic nodes, spleen, and liver. A refresh of staging system is summarized in Table 1.

This review describes the main differences between primary and secondary hepatic lymphoma, due to the common liver involvement as a part of the reticuloendothelial system. While secondary hepatic lymphoma (SHL) is commonly found in advanced cases, primary hepatic lymphoma (PHL) is a rare and poorly defined disease (Avlonitis and Linos 1999) and, hence, it is pivotal to characterize and differentiate these two entities (Salmon et al. 2006). The imaging manifestations of hepatic lymphoma, both in its primary and secondary form, are extremely variable and largely non-specific, but some features may serve as a useful diagnostic clue in the appropriate clinical setting.

Primary hepatic lymphoma

PHL is defined as a lymphoma localized and limited to the liver without evidence of involvement of other visceral organs, distant nodes, blood, and bone marrow for at least 6 months after the onset of hepatic disease (Caccamo et al. 1986; Kit Lei 1998). PHL represents the 0.016% of all NHL (Ugurluer et al. 2016) and commonly affects middle-aged individuals with a median age at diagnosis of 50 years and a male-to-female ratio of 2.3:1 (Peng et al. 2016). The Lugano Classification (Cheson et al. 2014) considers PHL as a limited extranodal disease without nodal involvement. The outcome of patients with PHL appeared much more favorable than that of patients with liver involvement by systemic lymphoma (Peng et al. 2016). However, survival rates for PHL vary considerably among reported cases, largely depending on comorbidity. The latter, especially immunosuppression, causes a large variation in survival ranging from 3 to 123.6 months (Steller et al. 2012).

Pathogenesis

PHL pathogenesis is not clear and many reports have suggested that it could evolve in immunocompromised patients and patients with a viral infection, hepatitis, and cirrhosis (Sutton et al. 1989; Honda et al. 1989; Rostaing et al. 1995). In all these situations, the possible inciting factor is the loss of T-cell surveillance and consequently the B-cell

Table 1 Revised staging system for primary nodal lymphomas (Leen et al. 2006)

Stage	Involvement	Extranodal (E) status
Limited I	One node or a group of adjacent nodes	Single extranodal lesions without nodal involvement
II	Two or more nodal groups on the same side of the diaphragm	Stage I or II by nodal extent with limited contiguous extranodal involvement
II bulky*	II as above with "bulky" disease	Not applicable
Advanced III	Nodes on both sides of the diaphragm; nodes above the diaphragm with spleen involvement	Not applicable
IV	Additional non-contiguous extra-lymphatic involvement	Not applicable

Extent of disease is determined by PET/CT for avid lymphomas and CT for non-avid histology. Tonsils, Waldeyer's ring, and spleen are considered nodal tissue. *Whether stage II bulky disease is treated as limited or advanced disease may be determined by histology and a number of prognostic factors

proliferation. Several recent reports have described an increased incidence of PHL in patients with HCV infection, which is particularly common, being found in 20–60% of PHL. The HCV genome does not get integrated into the host genome; therefore, malignant transformation probably occurs by indirect action: HCV is a lymphotropic virus and causes chronic B-cell stimulation leading to polyclonal and, eventually, monoclonal B-cell expansion (Vanita et al. 2005).

Histopathology

Although clinical features, laboratory data, and imaging studies may provide supportive evidence, PHL is a pathologic diagnosis. Tissue specimen can be obtained by fine-needle aspiration, percutaneous, laparoscopic, or open biopsy. The appearance, especially in a needle biopsy specimen, may be difficult to interpret but the diagnosis is very important as the prognosis is favorable. The destructiveness of the infiltrate in the liver biopsy is a very helpful feature to rule out benign inflammatory conditions, whereas immunocytochemistry is used to exclude an epithelial tumor, such as HCC (Noronha et al. 2005). PHL has been postulated to originate from Kupffer cells and transformed lymphocytes. Microscopically, the tumor cells may have a nodular or diffuse growth pattern. In the nodular form, the lymphoma cells have a destructive growth pattern, without detectable portal tracts within. In the diffuse variant, the hepatic architecture is preserved and the tumor cells infiltrate the portal tracts and may also extend along the sinusoids (Mastoraki et al. 2014) (Fig. 1).

NHL is the main histological subtype of PHL which can be classified as nodular (solitary or multiple lesions) or diffuse, often associated with hepatomegaly. Most PHL correspond to a larger cell type and demonstrate a B-cell immunophenotype. The predominant histological type is diffuse large B-cell lymphoma (80%) (Peng et al. 2016), while T-cell PHL is rare, representing approximately 5–10% of all PHL (Noronha et al. 2005). HL histology is extremely rare with very few case reports documented in the literature (Mastoraki et al. 2014).

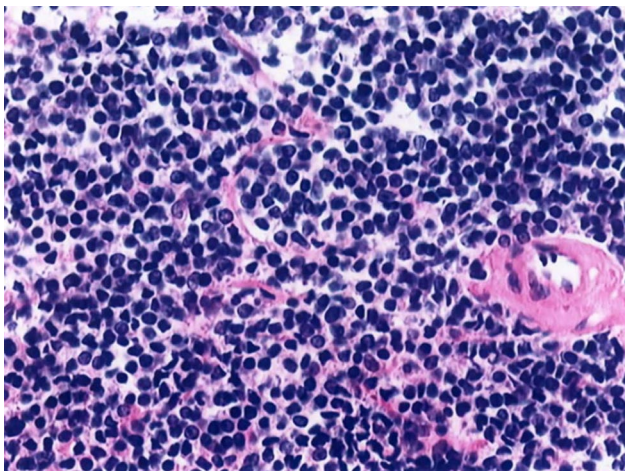

Fig. 1 Liver biopsy displaying monotonous sheets of small lymphocytes replacing normal hepatic parenchyma. Lymphocytes have scant cytoplasm with a clumped chromatin pattern and round nuclei (magnification 10×40) Noronha et al. (2005)

Clinical findings

Clinical presentation of PHL is usually non-specific with the most frequently reported symptom being abdominal pain in the right upper quadrant (occurring in 39–70% of patients), and constitutional symptoms such as fever, chills, anorexia, fatigue, malaise, nausea, and vomiting. B symptoms (fever and weight loss) occur in about one-third of the patients, whereas night sweats are less common (10%) (Vanita et al. 2005). Other symptoms include hemorrhagic diatheses such as epistaxis, gingival bleeding, and hematemesis (Aozasa et al. 1993) [Supplementary Table 1]. Hepatomegaly is present in 17% of patients, while splenomegaly is less common (10%). Spleen enlargement indicates a process other than PHL, but congestive splenomegaly can occur in PHL as a consequence of hepatic dysfunction and portal hypertension (Vanita et al. 2005). Finally, 10% of patients are asymptomatic with the diagnosis proven only after an evaluation for incidental hepatic abnormalities (Kit Lei 1998).

Laboratory findings

Blood counts are usually normal at an early stage of PHL. Liver function tests, including transaminases, alkaline phosphatase, and bilirubin, are abnormal in at least 70% of patients. Inflammatory markers, such as the erythrocyte sedimentation rate and C-reactive protein, are elevated in 30% of cases. Beta-2-microglobulin and lactate dehydrogenase are elevated in up to 80–90% of patients (Vanita et al. 2005), whereas αFP and CEA levels are usually normal. Other occasional laboratory findings include hypercalcemia (Santhosh-Kumar et al. 1990) and monoclonal paraproteinemia (Borgonovo et al. 1995).

Imaging findings

Most cases of PHL present with solitary or multiple liver mass that often mimics hepatocellular carcinoma. However, it may also present as diffuse hepatic involvement (Kit Lei 1998) [Supplementary table 2]. Due to its clinical and radiological resemblance to liver metastases of adenocarcinoma, PHL is frequently diagnosed intra- or post-operatively (Steller et al. 2012; Park and Jung 2017). A summary of the

Table 2 US, CT, and MRI findings useful to point out the main differential diagnosis between PHL and other focal liver lesions

	US	CT	MRI
PHL (single or multiple lesions)	Hypoechoic **Color-Doppler**: increased peripheral vascularity	**Unenhanced scan** → hypodense with a central area of lower density **Contrast-enhanced scan** → 50% no enhancement; 33% patchy enhancement in arterial phase and wash-out in portal-venous phase; 16%: peripheral ring of enhancement	**Unenhanced scan → T1:** hypointense; no signal drop on "out-of-phase" sequence **T2:** mildly hyperintense; occasionally with a highly hyperintense central scar **ADC:** low signal (cut-off value: $0.918 \times 10–3$ mm^2/s) **Contrast-enhanced scan with Gd-BOPTA** → arterial phase: shaded or mild ring-like enhancement; portal-venous phase: increasing patchy and heterogeneous enhancement; delayed phase: decreased enhancement; only septa are visible **Contrast-enhanced scan with Gd-EOB-DTPA** → hypointense in all phases
Metastasis	Hypoechoic (65%); round and well defined; mass effect with distortion of adjacent vessels; hypoechoic halo due to compressed and fat spared liver	**Unenhanced scan** → hypodense **Contrast-enhanced scan** → peripheral enhancement with a central area of lower density	**Unenhanced scan** **T1:** moderately hypointense **T2:** mildly-to-moderately hyperintense **Contrast-enhanced scan** → small lesions (< 1.5 cm): uniform enhancement; large lesions (> 1.5 cm): transient rim enhancement (i.e., with wash-out); perilesional enhancement: in colorectal and pancreatic adenocarcinoma metastasis
HCC	Small lesions hypoechoic; large lesions heterogeneous (necrosis and calcifications) **CEUS** → arterial phase: wash-in; portal venous-delayed phase: wash-out	**Contrast-enhanced scan** → arterial phase: rapid wash-in; portal venous-delayed phase: wash-out	**Unenhanced scan → T1:** hypointense; hyperintense if fat containing **T2:** mildly hyperintense **ADC:** low signal **Contrast-enhanced scan (BOPTA or EOB-DTPA)** → arterial phase: wash-in; portal venous-delayed phase: wash-out; hepatobiliary phase: hypointense
Abscess	Hypoechoic with hyperechoic foci Poorly demarcated **CEUS:** arterial phase: wall enhancement; portal venous- delayed phase wash-out	Central hypodense with peripheral hyperdense rim **Contrast-enhanced scan** → "double target sign": central hypodense lesion surrounded by a high attenuation inner rim and a low attenuation outer rim	**Unenhanced scan** → **T1:** hypointense and heterogeneous **T2:** hyperintense with perilesional oedema **ADC:** low signal within the cavity and high signal at the periphery **Contrast-enhanced scan** → enhancement of the capsule
Sclerosing hemangioma	Heterogeneously hyperechoic	**Unenhanced scan** → hypodense **Contrast-enhanced scan** → arterial phase: rim and nodular enhancement with peripheral transient hepatic attenuation difference; delayed phase: rarely homogeneous enhancement	**Unenhanced scan** → **T1:** hypointense; **T2:** variable (less hyperintense than typical hemangioma) **Contrast-enhanced scan** → arterial phase: absent or mild enhancement; delayed phase: mild peripheral enhancement

US ultrasound, *CT* computed tomography, *MRI* magnetic resonance imaging, *CEUS* contrast-enhanced ultrasound, *PHL* primary hepatic lymphoma, *HCC* hepatocellular carcinoma

imaging features by US, CT,0 and MRI of the most common differential diagnosis with PHL is provided in Table 2.

Ultrasound

As a rare disease, PHL can be detected incidentally during an abdominal US examination performed for a first evaluation or during surveillance in patients with risk factors for lymphoproliferative disorders. The typical US appearance is that of a large, solitary hypoechoic lesion or multiple hypoechoic lesions resembling metastasis. The hypoechoic texture is probably due to the high cellularity and lack of background stroma. PHL lesion can have increased peripheral vascularity, which can be depicted at Color-Doppler evaluation, thus mimicking hemangioma (Tomasian et al. 2015). Due to the non-specific US pattern, the overall accuracy of this imaging technique in PHL diagnosis can be limited (Hosten et al. 1999; González-Añón et al. 1999). CEUS has been increasingly used for the characterization of focal liver lesions (Dietrich 2012; Dietrich et al. 2012) showing a higher sensitivity and specificity (93% and 76%, respectively) compared to B-mode imaging (Tranquart et al. 2008). Hepatic lymphoma has not shown uniform behavior in the arterial phase among different studies (Brannigan et al. 2004; Leen et al. 2006; Foschi et al. 2010; D'Onofrio et al. 2015; Trenker et al. 2014), and thus, the late phase is considered the most useful, since almost all lesions seem to show wash-out. However, although no pathognomonic imaging feature exists on CEUS for hepatic lymphoma, the scarce marginal definition and irregularity of the lesion, suggesting an infiltrative growth, may represent a finding warranting focal biopsy (Foschi et al. 2010).

Computed tomography

The most common PHL presentation is a solitary lesion (55–60% of cases), followed by multiple lesions (35–40% of cases), while diffuse infiltration is uncommon. On unenhanced CT scans, PHL appears as a hypoattenuating lesion with a central low-density area suggesting necrosis. Following the administration of intravenous contrast medium, 50% of lesions do not enhance, 33% have a patchy enhancement, and 16% show a peripheral ring of enhancement. After chemotherapy, calcifications may develop within the lesions (Appelbaum et al. 2005). Most cases may mimic HCC with patchy enhancement in the arterial phase, hypodensity and hyperattenuating pseudocapsule in portal venous-delayed phase (Lee et al. 2017) (Fig. 2). Other differential diagnoses of PHL are represented by both benign lesions as sclerosing hemangioma and abscess, or malignant ones as cholangiocarcinoma or SHL in the "mass-like" variants when reaching huge dimensions. Indeed, these lesions may be characterized by a solid peripheral component with contrast enhancement and a central necrotic core determined by rapid cellular growth. The appearance of PHL may also be confused with other rare and poorly differentiated carcinomas, embryonal sarcoma, granulomatous cholangitis, inflammatory pseudotumor, or granulomatous hepatitis (van Leeuwen et al. 1996; Coakley et al. 1997).

Magnetic resonance imaging

MRI is mainly recommended as a third level-imaging technique in the work-up of patients with PHL and it is usually advocated to correctly characterize the incidental findings

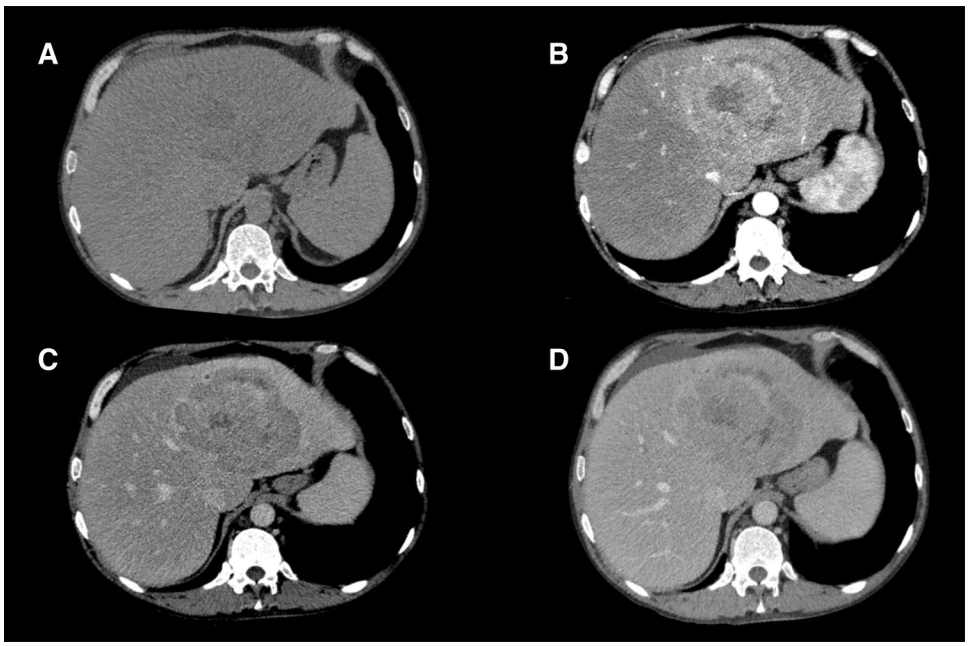

Fig. 2 CT scan of a 55-year-old male patient with diagnosis of PHL before and after intravenous injection of iodine contrast agent. **a** Unenhanced scan of a single mass located in S4, characterized by small hypoattenuating areas. **b** Arterial hepatic phase confirms the presence of an inhomogeneous lesion with peripheric hyperattenuating areas and hypoattenuating intralesional foci. **c** Portal-venous phase shows wash-out of hyperattenuating areas. **d** Delayed phase confirmed wash-out with peripheral rim enhancement (pseudocapsule)

of focal, multiple, or infiltrative disease. As mentioned above, the major differential diagnoses are represented by abscess and HCC (Noronha et al. 2005). Another possible misdiagnosis may be metastases and benign focal liver nodules, e.g., focal nodular hyperplasia (Noronha et al. 2005). To address the need to properly characterize suspicious focal liver lesions, standard MRI protocol should comprise: axial T1-weighted in- and out-of-phase breath-hold spoiled gradient-echo sequences, axial and coronal turbo-spin-echo respiratory-triggered and fat-suppressed T2-weighted sequences, diffusion-weighted images (DWI), and axial and coronal 3D T1-weighted fat-suppressed spoiled recalled-echo sequences before and after injection of gadolinium chelates contrast agent during arterial, portal-venous, delayed, and hepatobiliary phase. Through a PubMed search, using the keywords PHL and MRI, only 19 articles published between 2009 and 2019 were identified, of whom the majority were case reports (Mezzano et al. 2016; Leung et al. 2009). According to the revision of these reports, PHL mainly appears as a single, huge, and well-defined mass.

On unenhanced MRI scans, PHL is typically hypointense compared to adjacent liver parenchyma on T1-weighted images due to the presence of tissue different from healthy liver, without evidence of signal drop on "out-of-phase" sequence due to the absence of intracellular fat molecules.

On T2-weighted images, it is mildly hyperintense due to the presence of edema or necrosis, even if not so extensive. The presence of a central scar has been described and appears as highly hyperintense on T2-weighted sequences (Figs. 3, 4) (Nagata et al. 2015), similar to Focal Nodular Hyperplasia due to the presence of fibrosis.

The dynamic behavior after contrast media injection may vary and largely depends on the type of gadolinium chelates contrast agent injected. Usually, using extracellular contrast agents, not actively uptaken by hepatocytes, PHL shows a mild ring-like enhancement in the arterial phase, which increases in the portal-venous phase. Due to the huge dimension of the lesion, the enhancement is normally patchy and heterogeneous in this phase and, then, decreases in the delayed phase, during which only the septa, composed principally by fibrous tissue, are visible. The same dynamic

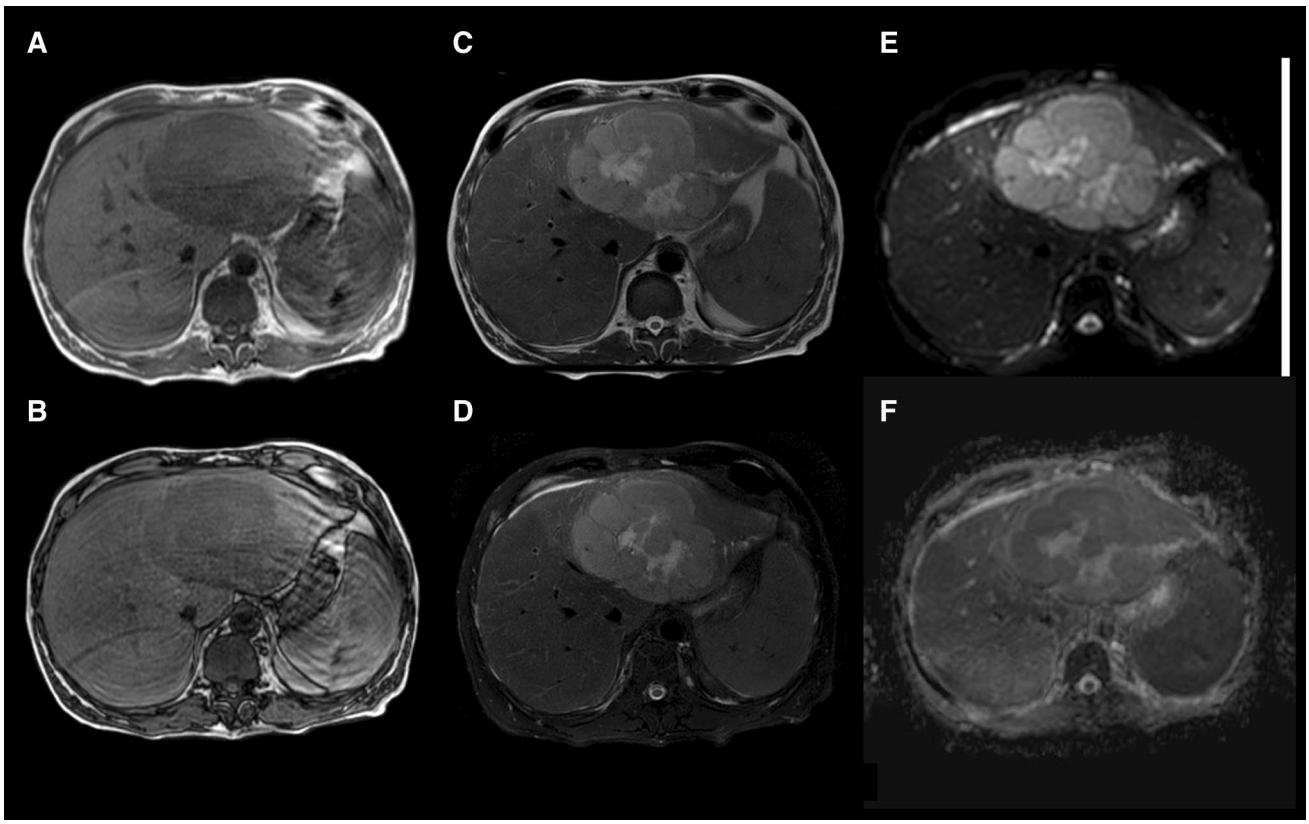

Fig. 3 MRI images of a 47-year-old male patient with diagnosis of PHL. **a**, **b** In- and out-phase T1W images of a hypointense mass located in the left lobe. **c**, **d** T2W images with and without fat suppression of PHL characterized by inhomogeneous signal hyperintensity with well-defined margins and a hyperintense central fibrous scar that should be differentiated from focal nodular hyperplasia. **e** DWI image confirms restricted diffusion of the lesion ($b = 800$). **f** The lesion appears hypointense on ADC map, due to real diffusion restriction

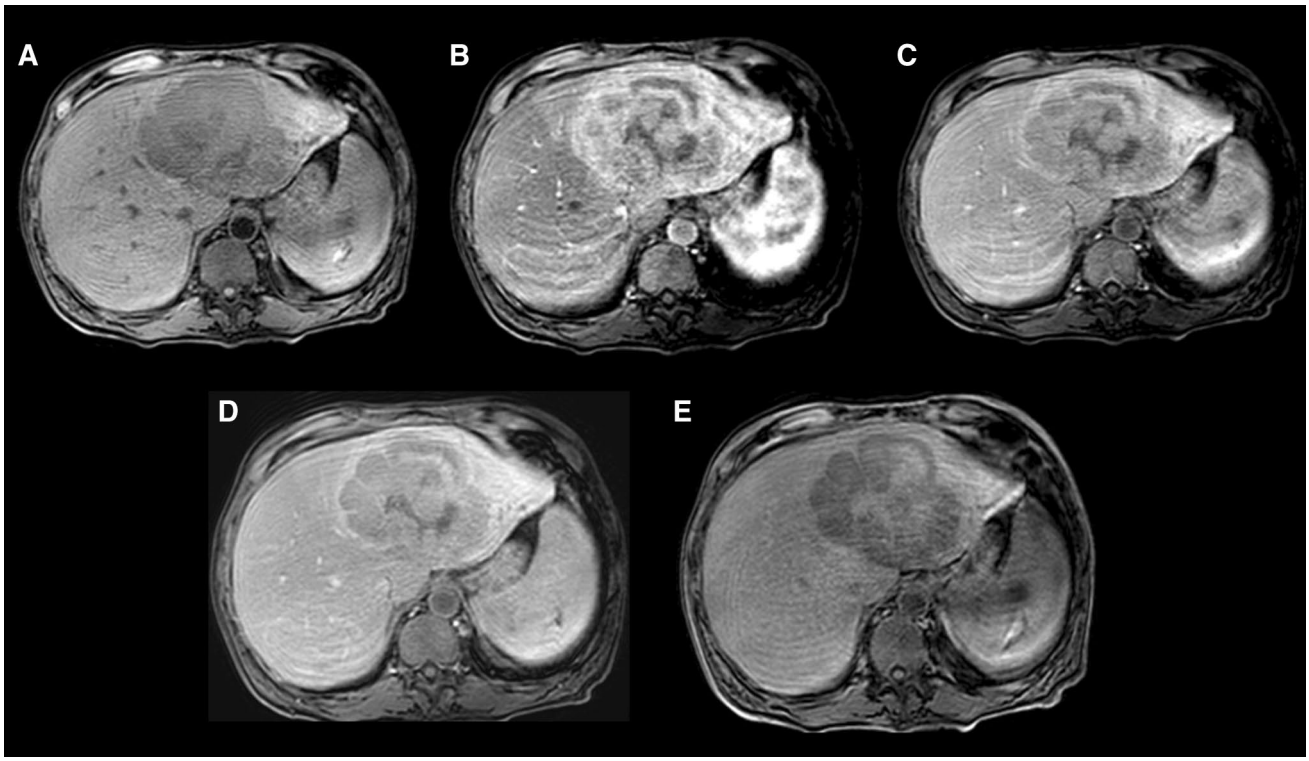

Fig. 4 MRI images of PHL shown in Fig. 3, before and after injection of hepatospecific contrast agent (Gd-EOB-DTPA). **a** Unenhanced T1 3D fat-sat scan shows a hypointense mass in the left lobe characterized by diffuse enhancement in arterial phase **b** with peripheral washout confirmed in portal-venous **c**—transitional phase **d** and peripheral rim enhancement. In hepatobiliary phase **e,** it is possible to appreciate the lesion's signal hypointensity

contrast behavior has been described using Gd-BOPTA (Multihance, Bracco) (Laroia et al. 2015; Dhamija et al. 2015). Instead, using Gd-EOB-DTPA (Primovist, Bayer), PHL remains hypointense in all dynamic phases. Despite both of these contrast agents are classified as hepatobiliary, this difference relies on their different pharmacodynamics properties. While only 5% of the injected Gd-BOPTA has a biliary excretion, approximately 50% of the injected Gd-EOB-DTPA is actively uptaken by Organic Anion Transporting Polypeptide 1 B1/B3-dependent hepatocyte and, then, excreted into the biliary drainage system through Multidrug Resistance-Associated Protein 2 (Gandhi et al. 2006). This behavior reflects the less evident enhancement during the dynamic phase of Gd-EOB-DTPA MRI studies. Nevertheless, with both contrast agents, PHL appears as hypointense in the hepatobiliary phase related to the absence of hepatocytes.

DWI is a very sensitive sequence for PHL, allowing its earlier identification due to the highly cellular nature of lymphoma that typically results in restricted diffusion (hyperintensity) with low ADC value (hypointensity) (Do et al. 2014; Leung et al. 2009). However, to the best of our knowledge, only one study performed a quantitative evaluation of ADC. According to the author, an ADC cut-off value of 0.918×10^{-3} mm^2/s has a sensitivity and specificity of 81.7% and 100%, respectively, in the differential diagnosis between PHL and other malignant lesion (Colagrande et al. 2018). Finally, whole-body DWI has been suggested to be as sensitive as PET for lymphoma staging (van Ufford et al. 2011), due to its capability of detecting lesions characterized by high cellularity. MRI features, compared to SHL, are summarized in Table 4.

Positron emission tomography (PET)

FDG PET-CT improves the accuracy of HL and FDG-avid NHL subtypes staging compared to CT for nodal and extranodal sites (Table 3). In HL, FDG PET-CT is more accurate than biopsy in the detection of bone marrow involvement. Therefore, if performed, bone marrow biopsy is no longer required (Cheson et al. 2014). A recent meta-analysis evaluating the accuracy of FDG-PET on lymphoma staging showed a sensitivity of 90% and specificity of 91% for this technique. Finally, PET-CT has shown to be more accurate than CT alone in restaging patients with HL or diffuse large B-cell lymphoma due to its superiority in detecting viable tumor from necrosis or fibrosis in residual masses (Cheson 2011). Furthermore, staging with PET-CT showed to

Table 3 US, CT, and MRI findings useful to point out the main differential diagnosis between SHL and other focal liver lesions

	US	CT	MRI
SHL	Single or multiple well-defined hypoechoic nodules Liver enlargement in diffuse involvement Normal in 25% Occasionally anechoic cystic lesion with septa	Single mass or multifocal hypodense lesions Hysodense to hepatic parenchyma in diffuse involvement Mass-like periportal low attenuation only in two cases	**Unenhanced scan → T1**: hypointense **T2**: mildly-to-moderately hyperintense **ADC:** low signal **Contrast-enhanced scan** → arterial phase: slightly to intensely homogeneous enhancement with peripheral hyperdense rim; portal venous-delayed phase: hypointense
Metastasis	Hypoechoic (65%); round and well defined; mass effect with distortion of adjacent vessels; hypoechoic halo due to compressed and fat spared liver	**Unenhanced scan** → hypodense **Contrast-enhanced scan** → peripheral enhancement with a central area of lower density	**Unenhanced scan → T1:** hypointense; hyperintense if fat containing **T2:** mildly hyperintense **ADC:** low signal **Contrast-enhanced scan (BOPTA or EOB-DTPA)** → arterial phase: wash-in; portal venous-delayed phase: wash-out; hepatobiliary phase: hypointense
CC	Hyperechoic	**Unenhanced scan** → homogeneous hypodense lesions **Contrast-enhanced scan** → peripheral enhancement with gradual centripetal enhancement Capsular retraction Intra-hepatic biliary ducts dilatation	**Unenhanced scan → T1:** moderately hypointense **T2:** moderately hyperintense **ADC:** peripherally hypointense target appearance **Contrast-enhanced scan** → arterial phase: hypointense; portal venous-delayed phase progressive centripetal enhancement

US ultrasound, *CT* computed tomography, *MRI* magnetic resonance imaging, *SHL* secondary hepatic lymphoma, *CC* cholangiocarcinoma

significantly decrease the mortality rate after 1 year from completion of the first-line therapy in patients with limited-stage aggressive NHL compared to patients treated for the limited-stage as determined by CT alone (Metser et al. 2019). The utility of PET-CT in the imaging of extranodal NHL involving various structures has been documented (Chan et al. 2008), confirming the absence of any additional focus of high uptake in the other parts of the body. However, in the setting of PHL, reports about imaging findings of FDG PET-CT are still scarce and mainly published as case reports. According to the most recent literature, PHL either as a single lesion, multiple nodules or infiltrative form, shows FDG uptake with a maximum Standardized Uptake Value ranging from 4.5 to 33.5 (Wang et al. 2020; Tang et al. 2018; Mahajan et al. 2016). As for other lymphomas, FDG PET-CT should be integrated into the work-up of patients with PHL to stage the disease, to evaluate treatment response, and to detect relapse and recurrence.

Secondary hepatic lymphoma (SHL)

SHL is relatively common and usually indicates advanced disease. It can occur in about 20% of patients with NHL and about 5% of patients with HL (Schiff et al. 2007). Secondary liver involvement is usually associated with node disease. While hepatic HL is almost invariably associated with splenic localization, hepatic NHL may occur in the absence of splenic lesions [Supplementary Table 1]. A summary of the imaging features by US, CT, and MRI of the most common differential diagnosis with SHL is provided in Table 3.

Histopathology

Lymphoma may be extranodal in approximately 40% of patients, due to the regional spread of nodal disease or hematogenous dissemination. At the time of presentation, liver involvement occurs in up to 15% of patients with NHL and 5% of patients with HL, the latter almost always with spleen involvement and typically with more advanced stages (Metser et al. 2004). Large cells (diffuse) and follicular B-NHL are the dominant histologic subtypes (Bach et al. 2012). Secondary liver involvement by lymphoma usually does not require a liver biopsy to reach a diagnosis (Cheson et al. 2014).

Clinical findings

Patients with SHL usually present with systemic B symptoms. Hepato-splenomegaly and generalized lymphadenopathy can be commonly found on systemic examination (Schiff et al. 2007). Rarely, patients with widespread systemic disease present with fulminant hepatic failure characterized by jaundice, encephalopathy, and coagulopathy (Lettieri and Berg 2003) [Supplementary Table 2].

Laboratory findings

Laboratory data include mild-to-moderate elevation of liver enzymes in almost all patients with systemic lymphoma due to tumor infiltration or extrahepatic bile duct obstruction, while αFP, CEA, and Carbohydrate Antigen 19.9 levels are normal in all patients (Schiff et al. 2007).

Imaging findings

Ultrasound

In SHL, ultrasound examination can be normal in up to 25% of cases or show a liver enlargement as exclusive finding. The recognized patterns of SHL in the US are small or large nodular lesions, mass, or diffuse infiltrating disease. Occasionally, SHL may appear as a target lesion (Wernecke et al. 1987) or an anechoic cystic lesion with septa (Townsend et al. 1989). In a published series, the most common sonographic findings were hepatomegaly and multiple, well-defined, hypoechoic nodular lesions, while the presentation as a single liver lesion was exceptional (Castroagudìn et al. 2007). This aspect can mimic metastatic disease from the other primary tumors and the differential diagnosis cannot be pointed out with US.

Computed tomography

The accuracy of CT in the detection of SHL is variable, with a reported sensitivity of 57% and specificity of 88% (Zornoza and Ginaldi 1981). Indeed, CT may not depict hepatic localization in cases presenting with small nodules (< 1 cm) or diffuse infiltration. Moreover, the liver texture may be irregular suggesting a benign parenchymal disease (e.g., fatty infiltration) other than tumor involvement.

CT appearance of SHL can be divided into three categories: (1) solitary hepatic mass, which may range in size from less than 1 cm to 10 cm, rarely shows calcifications unless the patient has undergone radiation therapy, and occasionally bleed (Fig. 5); (2) multifocal hepatic lesions, which may vary in size (typically are 1–5 cm) and are similar to metastatic disease (Fig. 6); (3) diffuse hepatic involvement, which is the most difficult to detect on CT, since lesions often show the same attenuation as hepatic parenchyma. In particular, the CT appearance of SHL may be indistinguishable from metastatic disease of any source (e.g., gastro-intestinal and gynecological cancer). One possible element of differentiation that should be considered is that metastases are characterized by a contrast

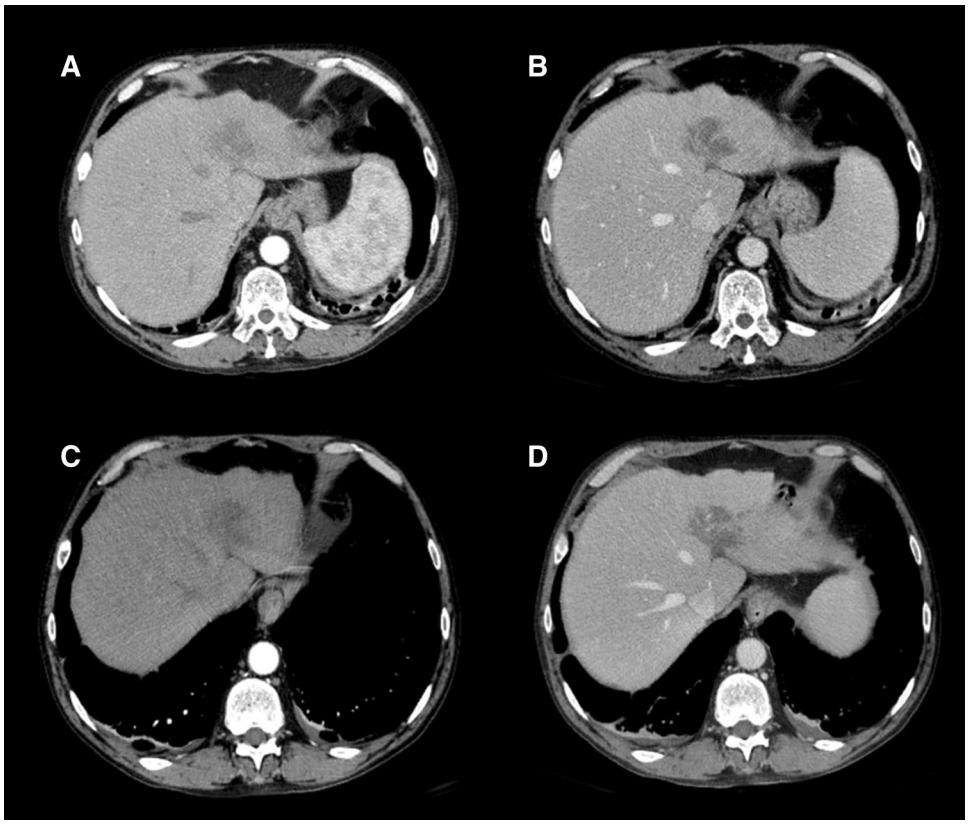

Fig. 5 Follow-up CT scans before and after intravenous injection of iodine contrast media of PHL shown in Figs. 3 and 4. Arterial and portal-venous phase during chemotherapy respectively after 3 (**a**, **b**) and 6 months (**c**, **d**) with dimensional reduction of the mass located in the left lobe

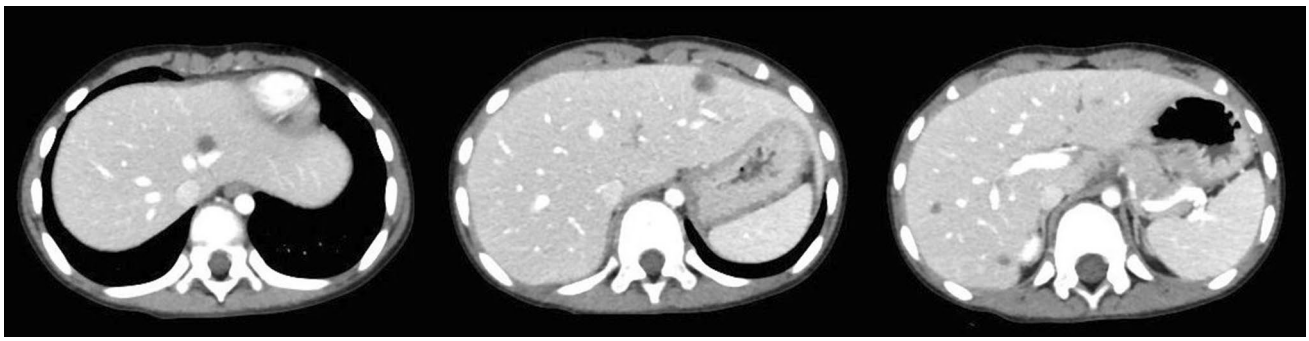

Fig. 6 CT scan after intravenous injection of iodine contrast media acquired in portal-venous phase of a 62-years old female patient with diagnosis of Hodgkin Lymphoma and secondary liver involvement. Portal-venous phase shows multiple hypoattenuating lesions located in S4 (left image), S2 (middle), and S7 and S8 (right)

enhancement behavior similar to the primary tumor. In this regard, SHL typically usually shows progressive enhancement with a peripheral rim in the delayed phase. Coakley et al. (1997) encountered two cases of NHL with an unusual pattern of hepatic involvement characterized by mass-like periportal infiltration. Mass-like periportal low attenuation is a rare finding with a limited number of described cases and should be differentiated from hilar cholangiocarcinoma. Hilar cholangiocarcinoma determines a retro-dilatation of the biliary tree, which is an important differential diagnosis tip from hepatic lymphoma. Moreover, cholangiocarcinoma tends to infiltrate the liver or the perihepatic structures, such as the portal vein or hepatic artery, determining liver vascular troubles (e.g., portal vein thrombosis). On CT scan, cholangiocarcinoma appears as a fibrous tissue that spreads into the biliary spaces from the hilum to the liver parenchyma with mild enhancement in arterial and portal-venous phase. During late acquisition (about 12–15 min), it appears hyperintense due to its fibrous tissue (contrast pooling).

Maher et al. (2001) demonstrated that the lymphomatous hepatic lesions showed lower attenuation than the normal liver. Rim enhancement following intravenous contrast was seen in only two cases and only one patient with a solitary lesion developed calcification after chemotherapy. Matsumoto et al. (2004) reported a case of diffuse involvement as a mass in the portal vein associated with mesenteric lymphadenopathy, which should be considered in the differential diagnosis of portal vein thrombus. Focal hepatic hypoattenuating lesions have various benign and malignant causes, and many are not readily characterizable on CT, particularly when smaller than 1 cm. In patients without known cancer, these lesions can be usually evaluated with serial follow-up or with other imaging modalities (e.g., MRI, PET-CT). In oncological patients, however, hepatic lesions may be pivotal for defining prognosis and therapy. In this regard, Schwartz et al. (1999) demonstrated that in a large population of patients with cancer, hepatic lesions measuring ≤ 1 cm are often benign (80.2%). However, these lesions could represent liver metastases in 11.6% of patients. This information could be useful to estimate the likelihood of metastatization; in particular a threshold growth, the presence of extrahepatic metastasis, and multiple liver lesions may account for metastatic disease.

Magnetic resonance imaging

With regards to SHL, no scientific study published in the last 10 years was found by matching the keywords SHL and MRI. This could be related to the easier diagnosis of SHL, since it arises as a secondary involvement of a primary lymphoma, typically of the spleen or nodes, usually appearing as multifocal lesions or diffuse infiltration of the liver. SHL shows a hypointense signal on T1-weighted sequence and a mild-to-moderate hyperintense signal on T2-weighted sequence. Contrast behavior may largely differ, but, contrary to PHL, it is usually homogenous. According to one of the most recent published studies regarding 11 lesions of SHL, the enhancement pattern depends on T2 signal intensity: lesions minimally hyperintense enhance slightly, while lesions moderately hyperintense enhance intensely (Kelekis et al. 1997). In both cases, the presence of a rim enhancement is common. The enhancement progresses through the other post-contrast phases, even if SHL lesions remain hypointense in comparison to the surrounding parenchyma. If a central fibrous scar is described, it presents a delayed, blood-pool, contrast enhancement: the source of collagen in pathological conditions is believed to be the stellate cells. Upon chronic liver injury, stellate cells are activated and transformed into a myofibroblast-like phenotype to lay down the extracellular matrix.

As PHL, SHL shows restricted diffusion with low ADC value; however, a cut-off value has not yet been identified and, therefore, further studies may be needed to correctly characterize SHL lesions.

MRI features, compared to PHL, are summarized in Table 4.

Positron emission tomography (PET)

Several studies have shown the value of PET-CT for staging, restaging, and therapy monitoring, especially in the evaluation of extranodal involvements (Buchpiguel 2011). The advantage of PET-CT is to detect extranodal sites that were previously missed at CT, most commonly within the liver and especially in case of small hypodense lesions (Metser et al. 2004; de Jong et al. 2009). Indeed, PET performed with non-enhanced CT is more sensitive and specific than contrast-enhanced CT alone for the evaluation of nodes and organ involvement. Table 5 summarizes utility and characteristics of diffuse lymphoma using FDG PET-CT in the evaluation of extranodal sites and Fig. 7 shows an example of liver involvement in a patient with NHL.

Table 4 MRI features of PHL and SHL

MRI sequence	PHL	SHL
T1-WI	Hypointense	Hypointense
T2-WI	Hyperintense Central scar: very hyperintense	Hyperintense Central scar: very hyperintense
Arterial phase	Mild enhancement Ring enhancement	Mild enhancement Ring enhancement
Portal-venous phase	Heterogeneous/patchy enhancement	Homogeneous enhancement
Delayed phase	Hypointense Septa: Hyperintense Central scar: hyperintense	Hypointense Central scar: hyperintense
DWI	Hyperintense	Hyperintense
ADC	Hypointense	Hypointense
Gd-EOB-DTPA	Hypointense in all sequences	Hypointense in all sequences

Arterial, portal-venous, and delayed phases after intravenous injection of Gd-BOPTA

Table 5 Criteria for involvement of site (Leen et al. 2006)

Tissue site	FDG Avidity	Test	Positive finding
Nodes	FDG-avid histology	PET-CT	Increased FDG uptake
	Non-avid disease	CT	Unexplained node enlargement
Spleen	FDG-avid histology	PET-CT	Diffuse uptake, solitary mass, miliary lesions, nodules
	Non-avid disease	CT	> 13 cm in vertical length, mass, nodules
Liver	FDG-avid histology	PET-CT	Diffuse uptake, mass
	Non-avid disease	CT	Nodules
CNS	FDG-avid histology or non-avid disease	CT	Mass lesion(s)
		MRI	Leptomeningeal infiltration, mass lesions
		CSF analysis	Cytology, flow cytometry
Other	FDG-avid histology or non-avid disease	PET-CT*, biopsy	Lymphoma involvement

*PET-CT is adequate for the determination of bone marrow involvement and can be considered highly suggestive for involvement of other extra-lymphatic sites. Biopsy confirmation of those sites can be considered if necessary

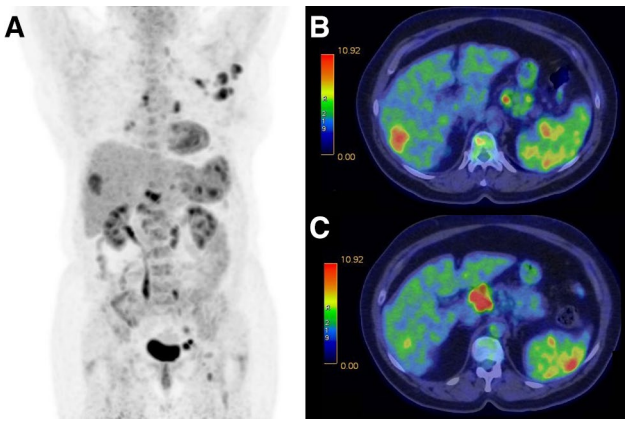

Fig. 7 FDG-PET imaging in a 70-year-old male patient with diagnosis of Non-Hodgkin Lymphoma. **a** Maximal intensity projection (MIP) image shows extensive sites of involvement visualized as areas of increased FDG uptake. **b**, **c** Fused PET-CT images show sites of liver involvement (S7), peripancreatic pathological nodes, and splenic uptake of FDG

Conclusions

Both PHL and SHL may be characterized using different radiological techniques. Imaging has a primary role in patients with clinical symptoms suggestive for lymphoproliferative disease, in particular, to evaluate which organs are affected and to establish a correct staging. In this background, both CT and MRI have showed a good correlation with histology, as they permit to distinguish between lymphomatous tissue, and necrotic and fibrotic areas. However, this correlation has been described only in few case reports and larger case series are needed to confirm it.

PHL should be distinguished first of all from liver involvement in diffuse lymphomatous diseases and other focal liver lesions, in particular HCC and metastasis. MRI plays a fundamental role in the differential diagnosis, especially between PHL and other focal liver diseases, using liver-specific contrast media and DWI, that is very sensitive in the identification of lymphoproliferative disorders due to its highly cellular nature. Moreover, FDG-PET may help the clinicians in the evaluation of focal uptake both in the liver and in other parts of the body.

Funding No funding has been received for this study

Compliance with ethical standards

Conflict of interest None of the authors have conflict of interests with this manuscript

Ethical approval This article does not contain any studies with human neither animal participants performed by any of the authors.

References

Appelbaum L, Lederman R, Agid R, Libson E (2005) Hepatic lymphoma: an imaging approach with emphasis on image-guided needle biopsy. Isr Med Assoc J 7:19–22

Armitage JO, Gascoyne RD, Lunning MA, Cavalli F (2017) Non-Hodgkin lymphoma. Lancet 390:298–310. https://doi.org/10.1007/s00432-020-03205-x

Avlonitis VS, Linos D (1999) Primary hepatic lymphoma: a review. Eur J Surg 165:725–729. https://doi.org/10.1080/11024159950189474

Aozasa K, Mishima K, Ohsawa M (1993) Primary malignant lymphoma of the liver. Leukemia Lymphoma 10:353–357. https://doi.org/10.3109/10428199309148560

Bach AG, Behrmann C, Holzhausen HJ et al (2012) Prevalence and imaging of hepatic involvement in malignant lymphoproliferative disease. Clinical Imaging 36:539–546. https://doi.org/10.1016/j.clinimag.2012.01.027

Borgonovo G, d'Oiron R, Amato A et al (1995) Primary lymphoplasmacytic lymphoma of the liver associated with a serum monoclonal peak of IgG kappa. Am J Gastroenterol 90:137–140
Brannigan M, Burns PN, Wilson SR (2004) Blood flow patterns in focal liver lesions at microbubble-enhanced US. Radiographics 24:921–935. https://doi.org/10.1148/rg.244035158
Buchpiguel CA (2011) Current status of PET/CT in the diagnosis and follow up of lymphomas. Rev Br Hematol Hemoter 33:140–147. https://doi.org/10.5581/1516-8484.20110035
Caccamo D, Pervez NK, Marchevsky A (1986) Primary lymphoma of the liver in the acquired immunodeficiency syndrome. Arch Pathol Lab Med 110:553–555
Castroagudìn JF, Molina E, Abdulkader I et al (2007) Sonographic features of liver involvement by lymphoma. J Ultrasound Med. 26:791–796. https://doi.org/10.7863/jum.2007.26.6.791
Chan WKS, Tse EWC, Fan Y-S et al (2008) Positron emission tomography/computed tomography in the diagnosis of multifocal primary hepatic lymphoma. J Clin Oncol 26:5479–5480. https://doi.org/10.1200/JCO.2008.18.5413
Cheson BD (2011) Role of functional imaging in the management of lymphoma. J Clin Oncol 29:1844–1854. https://doi.org/10.1200/JCO.2010.32.5225
Cheson BD, Fisher RI, Barrington SF et al (2014) Recommendations for Initial evaluation, staging, and response assessment of hodgkin and non- hodgkin lymphoma: the lugano classification. JCO 32:3059–3067. https://doi.org/10.1200/JCO.2013.54.8800
Coakley FV, O'Reilly EM, Schwartz LH et al (1997) Non-Hodgkin lymphoma as a cause of intrahepatic periportal low attenuation on CT. J Comput Assist Tomogr 21:726–728. https://doi.org/10.1097/00004728-199709000-00009
Colagrande S, Calistri L, Grazzini G et al (2018) MRI features of primary hepatic lymphoma. Abdom Radiol 43:2277–2287. https://doi.org/10.1007/s00261-018-1476-5
D'Onofrio M, Crosara S, De Robertis R et al (2015) Contrast-enhanced ultrasound of focal liver lesions. Am J Roentgenol 205:W56–W66
Dalrymple NC, Leyendecker JR, Oliphant M (2010) Problem solving in abdominal imaging with CD-ROM. Elsevier, Philadelphia, PA
de Jong PA, van Ufford HMQ, Baarslag H-J et al (2009) CT and 18F-FDG PET for noninvasive detection of splenic involvement in patients with malignant lymphoma. AJR Am J Roentgenol 192:745–753. https://doi.org/10.2214/AJR.08.1160
Dhamija E, Madhusudhan K, Shalimar et al (2015) Primary hepatic diffuse large B-cell lymphoma: unusual presentation and imaging features. Curr Probl Diagn Radiol 44:290–293. https://doi.org/10.1067/j.cpradiol.2014.12.002
Dietrich CF (2012) Liver tumor characterization–comments and illustrations regarding guidelines. Ultraschall Med 33(Suppl 1):S22–S30. https://doi.org/10.1055/s-0032-1312892
Dietrich CF, Cui XW, Schreiber-Dietrich DG, Ignee A (2012) EFSUMB guidelines 2011: comments and illustrations. Ultraschall Med 33(Suppl 1):S11–S21. https://doi.org/10.1055/s-0032-1312890
Do TD, Neurohr C, Michl M et al (2014) An unusual case of primary hepatic lymphoma mimicking sarcoidosis in MRI. Acta Radiol Short Rep 3:2047981613493625. https://doi.org/10.1177/2047981613493625
Elenitoba-Johnson KSJ, Lim MS (2018) New Insights into Lymphoma Pathogenesis. Annu Rev Pathol Mech Dis 13:193–217. https://doi.org/10.1146/annurev-pathol-020117-043803
Foschi FG, Dall'Aglio AC, Marano G et al (2010) Role of contrast-enhanced ultrasonography in primary hepatic lymphoma. J Ultrasound Med 29:1353–1356. https://doi.org/10.7863/jum.2010.29.9.1353
Gandhi SN, Brown MA, Wong JG et al (2006) MR contrast agents for liver imaging: what, when, how. Radiographics 26:1621–1636.https://doi.org/10.1148/rg.266065014
González-Añón M, Cervera-Deval J, García-Vila JH et al (1999) Characterization of solid liver lesions with color and pulsed Doppler imaging. Abdom Imaging 24:137–143. https://doi.org/10.1007/s002619900462
Honda H, Franken E et al (1989) Hepatic lymphoma in cyclosporine-treated transplant recipients: sonographic and CT findings. AJR Am J Roentgenol 152:501–503. https://doi.org/10.2214/ajr.152.3.501
Hosten N, Puls R, Bechstein W et al (1999) Focal liver lesions: Doppler ultrasound. Eur Radiol 9:428–435. https://doi.org/10.1007/s003300050687
Kelekis NL, Semelka RC, Siegelman ES et al (1997) Focal hepatic lymphoma: magnetic resonance demonstration using current techniques including gadolinium enhancement. Magn Reson Imaging. 15:625–636. https://doi.org/10.1016/s0730-725x(97)00111-2
Kit Lei KI (1998) Primary non-hodgkin's lymphoma of the liver. Leukemia Lymphoma 29:293–299. https://doi.org/10.3109/10428199809068566
Laroia ST, Rastogi A, Panda D, Sarin SK (2015) Primary hepatic non-hodgkin's lymphoma: an enigma beyond the liver, a case report. World J Oncol 6:338–344. https://doi.org/10.14740/wjon900w
Lee J, Park KS, Kang MH et al (2017) Primary hepatic peripheral T-cell lymphoma mimicking hepatocellular carcinoma: a case report. Ann Surg Treat Res 93:110–114. https://doi.org/10.4174/astr.2017.93.2.110
Leen E, Ceccotti P, Kalogeropoulou C et al (2006) Prospective multicenter trial evaluating a novel method of characterizing focal liver lesions using contrast-enhanced sonography. AJR Am J Roentgenol 186:1551–1559. https://doi.org/10.2214/AJR.05.0138
Leite NP, Kased N, Hanna RF et al (2007) Cross-sectional imaging of extranodal involvement in abdomino pelvic lymphoproliferative malignancies. Radiographics 27:1613–1634. https://doi.org/10.1148/rg.276065170
Lettieri CJ, Berg BW (2003) Clinical features of non-Hodgkin's lymphoma presenting with acute liver failure: a report of five cases and review of published experience. Am J Gastroenterol 98:1641–1646. https://doi.org/10.1111/j.1572-0241.2003.07536.x
Leung VKS, Lin SY, Loke TKL et al (2009) Primary hepatic peripheral T-cell lymphoma in a patient with chronic hepatitis B infection. Hong Kong Med J 15:288–290
Mahajan S, Kalra S, Chawla M, Dougall P (2016) Detection of diffuse infiltrative primary hepatic lymphoma on FDG PET-CT: hallmarks of hepatic superscan. World J Nucl Med 15(2):142–144. https://doi.org/10.4103/1450-1147.167581
Maher MM, McDermott SR, Fenlon HM et al (2001) Imaging of primary non-Hodgkin's lymphoma of the liver. Clin Radiol 56:295–301. https://doi.org/10.1053/crad.2000.0649
Mastoraki A, Stefanou MI, Chatzoglou E et al (2014) Primary hepatic lymphoma: dilemmas in diagnostic approach and therapeutic management. Indian J Hematol Blood Transfus 30:150–154. https://doi.org/10.1007/s12288-013-0263-2
Matsumoto S, Mori H, Takaki H et al (2004) Malignant lymphoma with tumor thrombus in the portal venous system. Abdom Imaging 29:460–462.https://doi.org/10.1007/s00261-003-0138-3
Metser U, Goor O, Lerman H et al (2004) PET–CT of extranodal lymphoma. Am J Roentgenol 182:1579–1586.https://doi.org/10.2214/ajr.182.6.1821579
Metser U, Prica A, Hodgson DC et al (2019) Effect of PET/CT on the management and outcomes of participants with hodgkin and aggressive non-hodgkin lymphoma: a multicenter registry. Radiology 290:488–495. https://doi.org/10.1148/radiol.2018181519
Mezzano G, Rojas R, Morales C et al (2016) Primary hepatic lymphoma: an infrequent focal liver tumour. Gastroenterol Hepatol 39:674–676. https://doi.org/10.1016/j.gastrohep.2015.09.008
Nagata S, Harimoto N, Kajiyama K (2015) Primary hepatic mucosa-associated lymphoid tissue lymphoma: a case report and literature

review. Surg Case Rep 1:87. https://doi.org/10.1186/s40792-015-0091-8
Noronha V, Shafi NQ, Obando JA, Kummar S (2005) Primary non-Hodgkin's lymphoma of the liver. Crit Rev Oncol Hematol 53:199–207. https://doi.org/10.1016/j.critrevonc.2004.10.010
Park J-I, Jung B-H (2017) Primary hepatic lymphoma treated with liver resection followed by chemotherapy: a case report. Ann Hepatobiliary Pancreat Surg 21:163–167. https://doi.org/10.14701/ahbps.2017.21.3.16
Peng Y, Qing AC, Cai J et al (2016) Lymphoma of the liver: clinicopathological features of 19 patients. Exp Mol Pathol 100:276–280. https://doi.org/10.1016/j.yexmp.2016.02.001
Rostaing L, Suc B, Fourtanier G et al (1995) Liver B-cell lymphoma after liver transplantation. Transplant Proc 27:1781–1782
Salmon JS, Thompson MA, Arildsen RC, Greer JP (2006) Non-Hodgkin's lymphoma involving the liver: clinical and therapeutic considerations. Clin Lymphoma Myeloma 6:273–280. https://doi.org/10.3816/CLM.2006.n.001
Santhosh-Kumar CR, Ajarim DS, Shipkey FD (1990) Primary non-Hodgkin's lymphoma of liver with humoral hypercalcaemia. Postgrad Med J 66:679–681. https://doi.org/10.1136/pgmj.66.778.679
Schiff ER, Sorrell MF, Maddrey WC (eds) (2007) Schiff's diseases of the liver, 10th edn. Lippincott Williams & Wilkins, Philadelphia
Schwartz LH, Gandras EJ, Colangelo SM et al (1999) Prevalence and importance of small hepatic lesions found at CT in patients with cancer. Radiology 210:71–74. https://doi.org/10.1148/radiology.210.1.r99ja0371
Shanbhag S, Ambinder RF (2018) Hodgkin lymphoma: a review and update on recent progress. CA: A Cancer J Clin 68:116–132. https://doi.org/10.3322/caac.21438
Steller EJ, Van Leeuwen MS, Van Hillegersberg R et al (2012) Primary lymphoma of the liver—a complex diagnosis. World J Radiol 4:53–57. https://doi.org/10.4329/wjr.v4.i2.53
Sutton E, Malatjalian D, Hayne OA, Hanly JG (1989) Liver lymphoma in systemic lupus erythematosus. J Rheumatol 16:1584–1588
Tang B, Li T-N, Ding C-Y (2018) (18)F-FDG PET/CT manifestation and clinical analysis of primary hepatic lymphoma. Zhongguo Shi Yan Xue Ye Xue Za Zhi 26(4):1062–1066. https://doi.org/10.7534/j.issn.1009-2137.2018.04.020
Tomasian A, Sandrasegaran K, Elsayes KM et al (2015) Hematologic malignancies of the liver: spectrum of disease. Radiographics 35:71–86. https://doi.org/10.1148/rg.351130008
Townsend RR, Laing FC, Jeffrey RB et al (1989) Abdominal lymphoma in AIDS: evaluation with US. Radiology 171:719–724. https://doi.org/10.1148/radiology.171.3.2655005
Tranquart F, Le Gouge A, Correas JM et al (2008) Role of contrast-enhanced ultrasound in the blinded assessment of focal liver lesions in comparison with MDCT and CEMRI: results from a multicentre clinical trial. Eur J Cancer Suppl 6:9–15. https://doi.org/10.1016/j.ejcsup.2008.06.003
Trenker C, Kunsch S, Michl P et al (2014) Contrast-enhanced ultrasound (CEUS) in hepatic lymphoma: retrospective evaluation in 38 cases. Ultraschall Med 35:142–148. https://doi.org/10.1055/s-0033-1350179
Ugurluer G, Miller RC, Li Y et al (2016) Primary hepatic lymphoma: a retrospective, multicenter rare cancer network study. Rare Tumors 8:118–123. https://doi.org/10.4081/rt.2016.6502
van Leeuwen MS, Noordzij J, Feldberg MA et al (1996) Focal liver lesions: characterization with triphasic spiral CT. Radiology 201:327–336. https://doi.org/10.1148/radiology.201.2.8888219
van Ufford HMEQ, Kwee TC, Beek FJ et al (2011) Newly diagnosed lymphoma: initial results with whole-body T1-weighted, STIR, and diffusion-weighted MRI compared with 18F-FDG PET/CT. AJR Am J Roentgenol 196:662–669. https://doi.org/10.2214/AJR.10.4743
Vanita N, Nelofar QS et al (2005) Primary non-Hodgkin's lymphoma of the liver. Elsevier, Amsterdam
Wang L, Dong P, Hu W et al (2020) 18F-fluoro-2-deoxy-D-glucose positron emission tomography/computed tomography in the diagnosis and follow-up of primary hepatic diffuse large B-cell Lymphoma: a clinical case report. Medicine (Baltimore) 99(5):e18980. https://doi.org/10.1097/MD.0000000000018980
Wernecke K, Peters PE, Kruger K (1987) Ultrasonographic patterns of focal hepatic and splenic lesions in Hodgkin's and non-Hodgkin's lymphoma. Br J Radiol 60:655–660. https://doi.org/10.1259/0007-1285-60-715-655
Zornoza J, Ginaldi S (1981) Computed tomography in hepatic lymphoma. Radiology 138:405–410. https://doi.org/10.1148/radiology.138.2.7455122